Progress in Chemical and Biochemical Research 2024, 7(1), 22-33

Progress in Chemical and Biochemical Research

Journal homepage: www.pcbiochemres.com

Original Research Article

The Impact of Sodium Dodecyl Sulfate on Methane Hydrate Volume Fraction in a Batch Rocking Cell Reactor

Abolfazl Mohammadi *

Department of Chemical Engineering, University of Bojnord, Bojnord, Iran

ARTICLEINFO

ARTICLEHISTORY

Submitted: 2023-10-22
Revised: 2023-11-08
Accepted: 2023-12-19
Available online: 2023-12-22
Manuscript ID: PCBR-2310-1301
Checked for Plagiarism: Yes
Language Editor: Dr. Fatimah Ramezani
Editor who Approved Publication: Dr. S. L. Sanati, Afsaneh

KEYWORDS

Methane
Gas Hydrates
Energy
Hydrate Volume Fraction
Conversion

ABSTRACT

Natural gas holds significant importance as a prospective energy source for meeting growing energy demands in the future. Gas hydrates offer a solution for the transportation and storage of natural gas. Within the sphere of gas hydrate formation, both the kinetics and thermodynamics play crucial roles and directly impact the economic feasibility of the process. In our current study, we focus on examining one specific kinetic parameter related to hydrate formation: the methane hydrate volume fraction (HVF) produced within a stirred batch reactor operating at a speed of 10 rpm. Our experiments were done out in a double-walled reactor with a capacity of 169 cm^3, maintaining a temperature of 275.15 K and a pressure of 7.5 MPa, utilizing a constant volume-constant temperature methodology. The experimental findings indicated that the utilization of SDS, noticeably, increases the amount of water to hydrate conversion, and the amount of combined volume of unreacted water and formed hydrate during hydrate growth. The addition of 350 ppm and 700 ppm SDS resulted in an increase in HVF by 491.2% and 495.7%, respectively, after 1 hour of hydrate growth.

Citation: A. Mohammadi*. The Impact of Sodium Dodecyl Sulfate on Methane Hydrate Volume Fraction in a Batch Rocking Cell Reactor. Prog. Chem. Biochem. Res., 7(1) (2024) 22-33
https://doi.org/10.48309/pcbr.2024.421942.1301
URL: https://www.pcbiochemres.com/article_185775.html

* Corresponding author: Abolfazl Mohammadi
✉ E-mail: mohammadi.a@ub.ac.ir
☏ Tel number: +989355012219

GRAPHICAL ABSTRACT

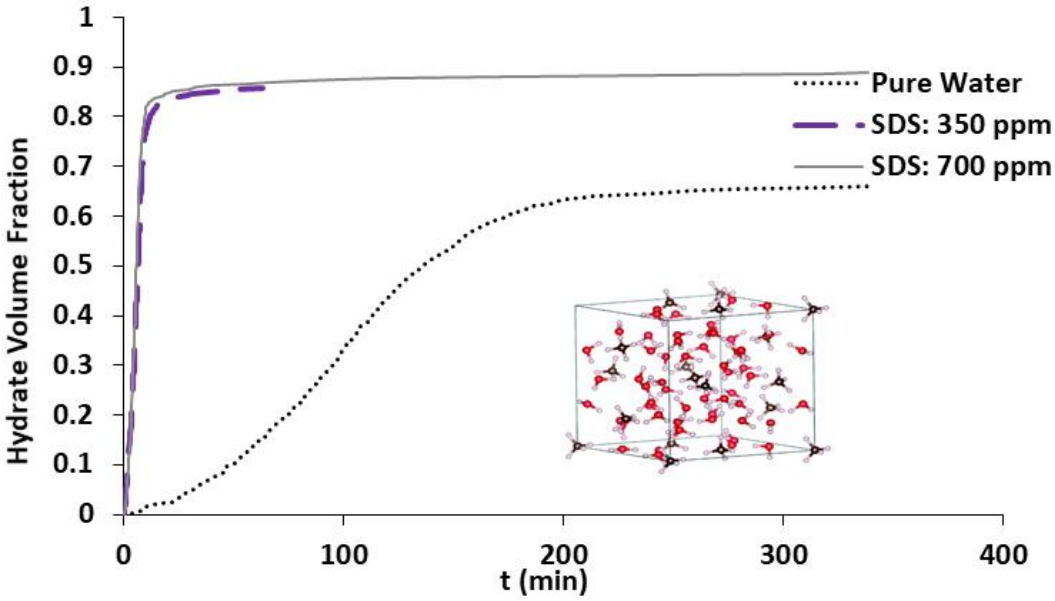

Introduction

In recent decades, there has been a substantial increase in the need for natural gas, primarily driven by its recognized environmental benefits, energy efficiency, and versatility as a fuel source. To accommodate this escalating demand, there has been a parallel expansion in the development of a resilient transportation infrastructure, facilitating the movement of natural gas across vast geographical expanses. There are some methods of transporting natural gas like pipelines, compressed natural gas (CNG), liquified natural gas (LNG), and the conversion of gas to liquids (GTL). Nonetheless, the constraints and issues linked to these conventional approaches have encouraged the exploration of substitute technologies [1-11]. Natural gas hydrates (NGH), which are firm crystalline substances comprising water and gas molecules, have attracted interest due to their capacity to potentially transform the natural gas transportation landscape [12-15]. Natural gas hydrates provide an effective method for the long-distance transportation of gas. Their notable energy density establishes them as a favorable choice for the storage and conveyance of gas. Gas hydrates, sometimes referred to as clathrate hydrates, are structured like ice crystals, arising from the entrapment of gas molecules within water molecule cages. This phenomenon materializes at low temperatures and high pressures, facilitated by hydrogen bonding among water molecules. These molecular cages can accommodate suitably sized molecules [16-18]. Lately, researchers have been exploring practical uses of gas hydrates in diverse fields, including the storage and conveyance of natural gas [19,20], desalination of saline water [21,22], greenhouse gas sequestration [23,24], serving as a cold storage medium [25,26], and concentrating juices and coffee [27,28]. Nevertheless, the extended initiation time, sluggish growth of hydrate formation, and the substantial pressure requirements pose significant obstacles, hindering the widespread production of gas hydrates. One effective approach to surmounting these challenges is the application of kinetic and thermodynamic enhancers [29-37]. Javanmardi *et*

al. (2005) conducted a study to determine the overall capital investment, operational expenses, maintenance costs, and the complete expenses associated with producing natural gas hydrates. Their research delved into how various operational factors influenced the economic aspects of transporting natural gas hydrate from Asaluyeh port in southern Iran to diverse gas markets [12]. Zhang *et al.* studied the impact of sodium dodecyl sulfate on methane hydrate formation within a nonstirred batch reactor. Their findings revealed that the inclusion of SDS effectively decreases the induction time. However, no consistent pattern emerged between induction times and varying SDS concentrations [38]. Liu *et al.* conducted a comparative analysis to assess the kinetic promotion effects of sodium dodecyl sulfate and L-methionine (L-Met) on CO_2 hydrate formation. The results from their experiments demonstrated that L-Met significantly enhances the formation of CO_2 hydrates, with a gas uptake in CO_2 hydrate formation being five times higher compared to SDS at equivalent concentrations [39]. In a study conducted by Sun *et al.*, a comparison was made between the effectiveness of anionic sodium dodecyl sulfate (SDS) and dodecyl polysaccharide glycoside (DPG) in promoting CH_4 hydrate formation. The results indicated that SDS outperformed DPG in terms of both the hydrate formation rate and storage capacity [40]. In another investigation by Ugur Karaaslan *et al.*, the promotion efficiency of different surfactants on natural gas hydrate formation was examined. The findings revealed that the anionic surfactant linear alkyl benzene sulfonic acid exhibited superior promotion efficiency compared to the quaternary ammonium salt and nonionic nonylphenol ethoxalate [41]. In 202, Mohammadi *et al.* conducted a study to explore the impact of SDS and tetra n-butylammonium fluoride on the kinetic parameters of methane hydrate formation. Their findings indicated that when SDS and tetra n-butylammonium fluoride were used simultaneously, it had an adverse effect on the kinetics of hydrate formation, as opposed to the results observed with TBAF and SDS solutions [25]. Researchers also employed nano-fluids characterized by high thermal conductivity to enhance the process of gas hydrate formation [29,42-46]. In a study conducted by Arjang *et al.*, silver nanoparticles were utilized to enhance methane hydrate formation at pressures of 4.7 and 5.7 MPa. The results demonstrated that compared to pure deionized water, the presence of nano-silver led to a reduction in the induction time by 85% and 73.9%, respectively, at the aforementioned pressures. In addition, the gas consumption was improved by 33.7% and 7.4% under the same conditions [44].

The hydrate volume fraction (HVF) is a kinetic parameter that represents the volume fraction of formed hydrate in an aqueous solution. This parameter has garnered limited attention from researchers. The aim of this study is to examine the impact of different concentrations (350 and 700 ppm) of SDS on the hydrate volume fraction during the process of methane hydrate formation.

Experimental

Materials

In the hydrate formation experiments, we employed double-distilled water as the primary solvent. The methane gas utilized in these tests was sourced with a 99.95% purity level and was procured from Kavian Gas Company. We acquired SDS, with a purity of 98 wt%, from Sigma-Aldrich Merck Company. The chemical structure of SDS is depicted in Fig 1.

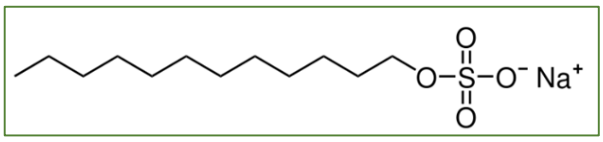

Fig 1.SDS chemical structure

The methane gas was stored in a 50-liter container, initially pressurized at 16.5 MPa.

2.2. Apparatus and Procedure

To facilitate our experiments, we employed a jacketed stainless-steel reactor constructed from SS-316, boasting a 169 cm^3 internal capacity and capable of withstanding an operational pressure of 200 bar. Within this reactor's inner chamber, four valves were installed; each rated at a pressure tolerance of 6000 psi. Two of these valves were ball valves, serving the purpose of injecting the solution and discharging the water-gas mixture post-experiment.

The remaining two valves were needle valves, one facilitating gas injection, and the other serving as a connection point to a gas chromatograph device for gas sampling. We integrated two ports into the reactor's outer wall. These ports allowed for the entry and exit of a cooling fluid, thus affording precise temperature control within the reactor. Our choice for the coolant was a 30% weight solution of ethylene glycol. To minimize energy loss, we took measures to insulate the reactor, connections, and fluid transfer pipes effectively. To monitor the internal temperature of the reactor, we utilized a Pt-100 platinum temperature sensor with an accuracy level of ±0.1 K. For reservoir pressure measurements, we employed a BD type pressure sensor with an accuracy of approximately 0.1 MPa. To ensure proper mixing within the primary hydrate formation chamber, an autoclaving stirrer was implemented, while a vacuum pump was utilized to create a vacuum inside the cell. A photo of the hydrate formation apparatus employed in this research is depicted in Fig 2.

Results and Discussion

At the commencement of each kinetic hydrate formation experiment, the cell is subjected to a cleansing procedure involving tap water followed by distilled water. Subsequently, the interior of the reactor is evacuated of air by means of a vacuum pump, and 25 cm^3 of the solution is introduced into the cell. The reactor's temperature is precisely set at 275.15 Kelvin via a temperature bath.

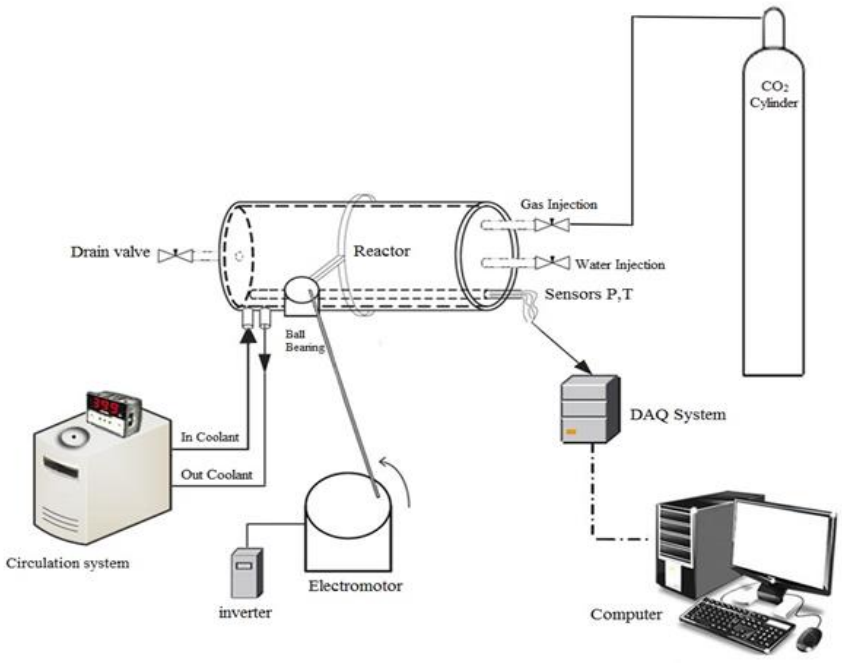

Fig 2. Visual representation of the experimental apparatus

Table 1. The Langmuir constant parameters, critical properties, and acentric factor for methane

Gas	A_{Small} (K/MPa)	B_{Small} (K)	A_{large} (K/MPa)	B_{large} (K)	P_c (MPa)	T_c (K)	ω
CH_4	7.228×10^{-4}	3187	2.335×10^{-2}	2653	4.599	190.56	0.0114

The hydrate-forming gas, in this case, methane, is introduced into the cell until the desired pressure is attained. Following this, the electromotor is activated and adjusted to a speed of 10 rpm.

Over a certain duration, hydrate formation initiates, leading to a decrease in system pressure until it reaches a state of stability where fluctuations within the reactor become minimal (0.05 bar/hr). The quantification of gas uptake is accomplished through the utilization of the Peng-Robinson equation of state [47]. Throughout the hydrate formation process, temperature and system pressure readings are gathered on a computer. The physical interaction between water and gas, in the context of hydrate formation can be described as follows:

$$CH_4 + MH_2O \longleftrightarrow CH_4 \bullet MH_2O \quad (1)$$

Where, M represents the hydration number [48].

$$M = \frac{46}{6\theta_L + 2\theta_S} \quad (2)$$

Within this formula, the variables θ_S and θ_L denote the fractional occupancy of small (S) and large (L) cages, respectively. The computation of these parameters is carried out in accordance with the principles of Langmuir adsorption theory, as detailed below [48]:

$$\theta_i = \frac{C_i f_{CH_4}}{1 + C_i f_{CH_4}} \quad (3)$$

The Langmuir constants for both large and small methane hydrate cavities are presented in Table 1.

The PR EoS is written as follows [47]:

$$P = \frac{RT}{v-b} - \frac{a}{v^2 + 2bv - b^2} \quad (4)$$

Within Equation (4), the variables "a" and "b" represent the energy and volume characteristics, respectively. The particulars of the PR EoS parameters are outlined below:

$$a = 0.45724 \frac{(RT_c)^2}{P_c} \alpha(T) \quad (5)$$

$$b = 0.0778 \frac{RT_c}{P_c} \quad (6)$$

Within Equations (5) and (6), "v" represents the molar volume. The expression for the PR EOS parameter is articulated as follows:

$$\alpha(T) = (1 + m(1 - T_r^{0.5}))^2 \quad (7)$$

$$m = 0.37464 + 1.54226\omega - 0.26992\omega^2 \quad (8)$$

Due to variations in molar volumes between the solution and gas hydrate, the gas volume within the cell diminishes as gas hydrate forms and expands. Consequently, we can calculate the instantaneous gas volume within the cell, labeled as V_t, using the subsequent equation [48]:

$$V_t = V_{cell} - V_{S_0} + V_{RW_t} - V_{H_t} \quad (9)$$

Where, V_{cell} and V_{s0} denote the cell volume (169 cm^3) and the initial volume of the feed solution (25 cm^3), respectively. In addition, V_{RWt} and V_{Ht} represent the volume of reacted water and the volume of produced hydrate, respectively. The subscript "t" in the equation signifies the time-dependent nature of these parameters.

The calculation for the volume of the converted water is determined using the subsequent equation [48]:

$$V_{RWt} = M \times \Delta n_{CH_4} \times \upsilon_w^L \quad (10)$$

The molar volume of aqueous solution, denoted as υ_w^L, is computed using Equation (11) [48]:

$$\upsilon_w^L = 18.015 \times \{1 - (1.0001 \times 10^{-2}) + (1.33391 \times 10^{-4})[1.8(T - 273.15) + 32] + (5.50654 \times 10^{-7})[1.8(T - 273.15) + 32]^2\} \times 10^{-3} \quad (11)$$

Where, T (temperature) and υ_w^L are represented in K (Kelvin) and m^3/kmol (cubic meters per kilomole), respectively. For structure sI empty hydrate lattice, υ_w^L, V_{H_t}, and conversion can be obtained from the following equations [48]:

$$\upsilon_w^{MT}[I] = (11.835 + 2.217 \times 10^{-5} T + 2.242 \times 10^{-6} T^2)^3 \frac{10^{-30} N_A}{46} - 8.006 \times 10^{-9} P + 5.448 \times 10^{-12} P \quad (12)$$

$$V_{H_t} = M \times \Delta n_{CH_4} \times \upsilon_w^{MT} \quad (13)$$

$$Conv = \frac{M \times \Delta n_{CH_4}}{n_{W_0}} \quad (14)$$

The hydrate volume fraction, HVF, is evaluated by the following equation [49]:

$$HVF = \frac{V_{H_t}}{V_{H_t} + V_{S_t}} \quad (15)$$

Table 2 presents the calculated values for water to hydrate conversion in SDS (350 ppm and 700 ppm) solutions. After 1 hour of hydrate growth, the water to hydrate conversion amount were calculated as 12.02%, 82.75%, and 83.73% in pure water, SDS (350 ppm) solution, and SDS (700 ppm) solution, respectively. It is evident that the SDS utilization at concentrations of both 350 ppm and 700 ppm significantly enhances the conversion of water to hydrate. According to research findings, SDS stands out as one of the most effective gas hydrate formation promoters [38-39,50-51]. SDS, as an anionic surfactant, reduces the surface tension of water molecules, leading to an increased gas uptake both in terms of quantity and rate. Fig.s 3 and 4 illustrate the SDS influence on the volume of the remaining solution and the formed of hydrate during methane hydrate growth. As can be seen in these figures as the reaction of hydrate formation proceeds, the volume of unreacted water decreases, and the volume of hydrate increases. As can be found from Figs. 3 and 4, the disparity in molar volume between water and the formed hydrate results in the combined volume of unreacted water and formed hydrate exceeding the initial volume of the injected solution (25 cc). Following 1 hour of hydrate growth in a pure water solution, the volume of unreacted water and formed hydrate were recorded as 22.03 mL and 3.734 mL, respectively.

Table 2. The effect of SDS on the water to hydrate conversion during hydrate growth at P_0 = 7.5 MPa and T = 275.15 K

System	Conversion at t=5 min	Conversion at t=10 min	Conversion at t=20 min	Conversion at t=60 min	Conversion at t=200 min
Pure water	0.4	1.23	1.95	12.02	57.79
Water + SDS (350 ppm)	28.31	72.81	79.99	82.75	82.78
Water + SDS (700 ppm)	31.74	77.75	81.66	83.73	85.57

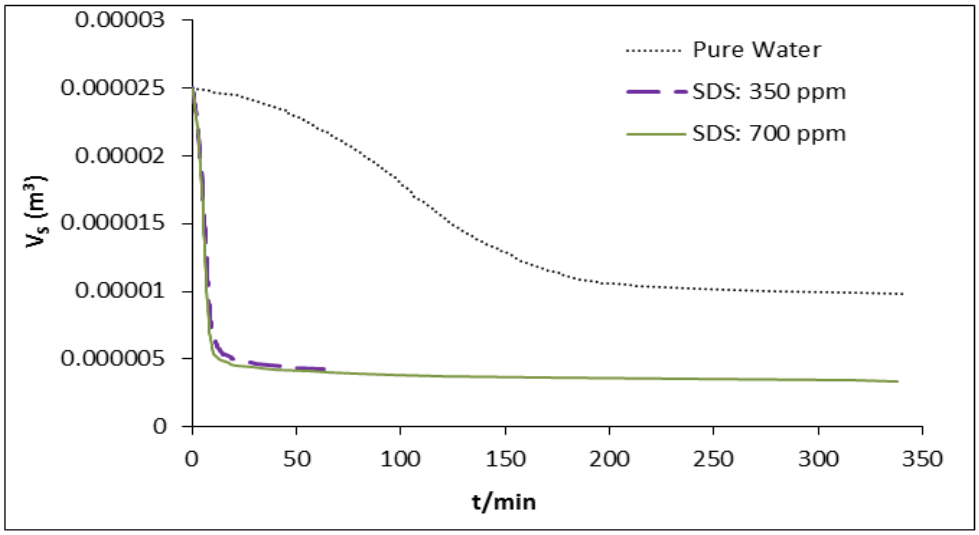

Fig 3. The volume of remained solution versus time in methane hydrate formation process at P_0 = 7.5 MPa and T = 275.15 K

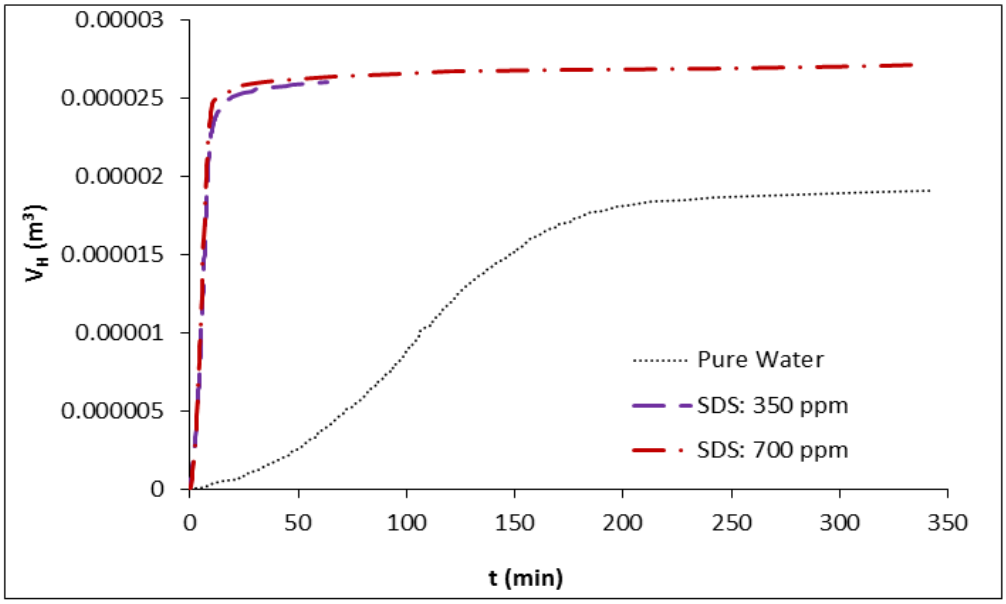

Fig 4. The volume of formed hydrate vs. time in methane hydrate formation process at P_0 = 7.5 MPa and T = 275.15 K

Table 2. The effect of SDS on the hydrate volume fraction (HVF) during hydrate growth at 7.5 MPa and 275.15 K

System	HVF at t=5 min	HVF at t=10 min	HVF at t=20 min	HVF at t=60 min	HVF at t=200 min
Pure water	0.01	0.02	0.02	0.15	0.63
Water + SDS (350 ppm)	0.33	0.77	0.83	0.86	0.86
Water + SDS (700 ppm)	0.37	0.82	0.85	0.86	0.88

In pure water, the combined volume of unreacted water and formed hydrate reached 25.77 cc.
Conversely, in the presence of SDS at concentrations of 350 ppm and 700 ppm, the respective combined volumes were measured as 30.33 cc and 30.38 cc. It is evident that the SDS utilization significantly increases the combined volume of unreacted water and formed hydrate when compared to the initially injected solution.
Table 3 presents the impact of SDS with concentrations of 350 ppm and 700 ppm on the hydrate volume fraction (HVF) during hydrate growth. These findings are also visualized in Fig 5. As depicted in Fig 5 and Table 3, the utilization of both SDS concentrations leads to a significant increase in HVF compared to pure water.

Fig 6 displays the calculated HVF values at different times during methane hydrate growth (t= 5, 10, 20, 60, and 200 min) under an initial pressure of 7.5 MPa and a temperature of 275.15 K. As evident from the figure, the use of 350 and 700 ppm SDS significantly enhances HVF within the first hour of hydrate growth. After 20 minutes of hydrate growth, HVF values were calculated as 0.0238 in pure water, 0.8347 in the SDS (350 ppm) solution, and 0.8487 in the SDS (700 ppm) solution. This indicates a noticeable enhancement in HVF when SDS is present. Furthermore, the SDS utilization with concentrations of 350 ppm and 700 ppm resulted in an increase in HVF by 491.2% and 495.7%, respectively, after 1 hour of hydrate growth, compared to pure water.

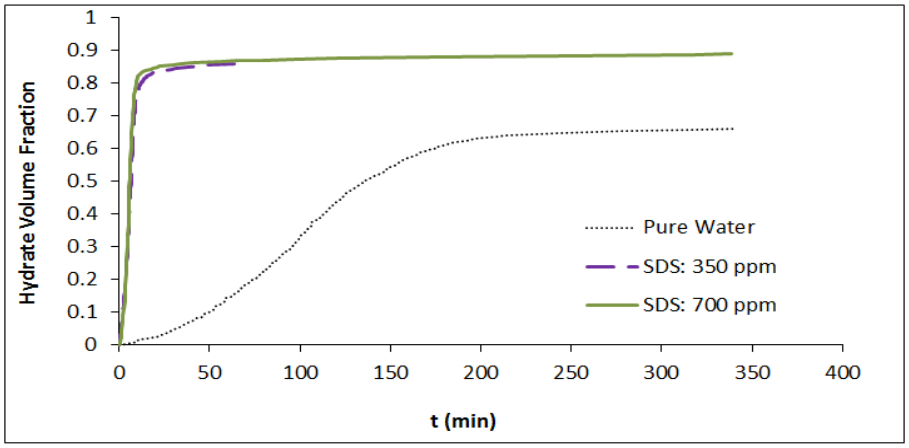

Fig 5. The amount of hydrate volume fraction vs. time in methane hydrate formation process at P_0 = 7.5 MPa and T = 275.15 K

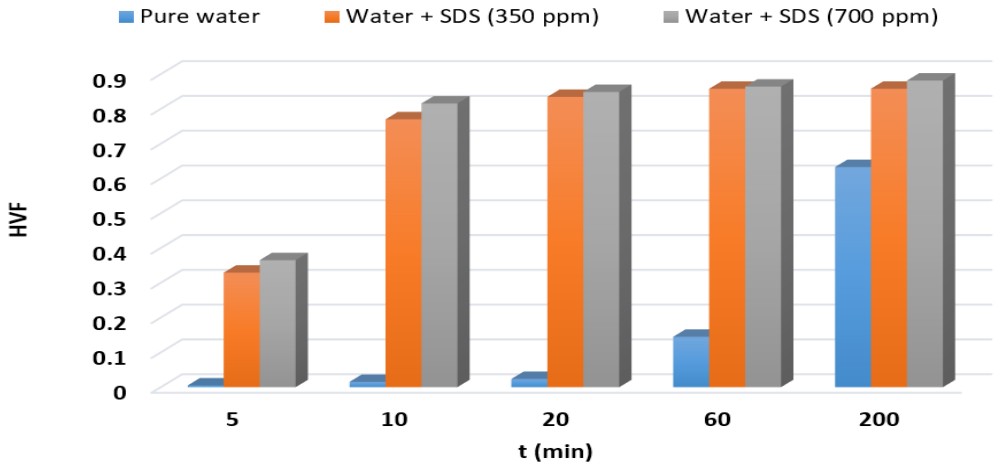

Fig 6. The effect of SDS on the quantities of hydrate volume fraction at various times of the methane hydrate growth at P_0 = 7.5 MPa and T = 275.15 K

The SDS utilization reduces the surface tension of water molecules, resulting in an accelerated hydrate formation process. This increase in hydrate formation process leads to a greater quantity of formed hydrate, ultimately enhancing both water to hydrate conversion and HVF.

Conclusion

The amount of water to hydrate conversion and hydrate volume fraction were calculated in aqueous solutions of SDS (350 ppm and 700 ppm). The experimental findings indicated that when compared to using only pure water, the inclusion of 350 and 700 ppm SDS led to a significant boost in HVF, with increments of 491.2% and 495.7%, respectively. Utilization of SDS, noticeably, increases the amount of water to hydrate conversion, and the amount of combined volume of unreacted water and formed hydrate during hydrate growth.

ORCID

Abolfazl Mohammadi
0000-0002-0623-4815

Funding

The authors declare that no funds, grants, or other support were received during the preparation of this manuscript.

Declarations

Conflict of interest: The authors have no relevant financial or non-financial interests to disclose.
Ethical approval: Not applicable.
Consent to participate: Not applicable.
Consent for publication: Not applicable

References

1. Shaton K, Hervik A, Hjelle HM. The environmental footprint of natural gas transportation: LNG vs. pipeline, *Economics of Energy & Environmental Policy*; 2020; 9(1). [Crossref], [Google scholar], [Publisher]
2. Cao M, Gai T, Xing Y, Liu Y, Wu J. Risk management of liquefied natural gas transportation routes: An interactive consensus reaching approach under personalized individual semantics, *Computers & Industrial Engineering*; 2022 Jul 1; 169:108307. [Crossref], [Google scholar], [Publisher]
3. Miana M, Del Hoyo R, Rodrigálvarez V, Valdés JR, Llorens R. Calculation models for prediction of Liquefied Natural Gas (LNG) ageing during ship transportation, *Applied Energy*; 2010 May 1; 87(5):1687-700. [Crossref], [Google scholar], [Publisher]
4. Ríos-Mercado RZ, Borraz-Sánchez C. Optimization problems in natural gas transportation systems: A state-of-the-art review, *Applied Energy*; 2015 Jun 1; 147:536-55. [Crossref], [Google scholar], [Publisher]
5. Khan MI, Yasmin T, Shakoor A. Technical overview of compressed natural gas (CNG) as a transportation fuel, *Renewable and Sustainable Energy Reviews*; 2015 Nov 1; 51:785-97. [Crossref], [Google scholar], [Publisher]
6. Thomas S, Dawe RA. Review of ways to transport natural gas energy from countries which do not need the gas for domestic use, *Energy*; 2003 Nov 1; 28(14):1461-77. [Crossref], [Google scholar], [Publisher]
7. Wood DA, Nwaoha C, Towler BF. Gas-to-liquids (GTL): A review of an industry offering several routes for monetizing natural gas, *Journal of Natural Gas Science and Engineering*; 2012 Nov 1; 9:196-208. [Crossref], [Google scholar], [Publisher]
8. O. Ajagbe. (2019). [Crossref], [Google scholar], [Publisher]
.9. U.J. Obibuike, S.T. Ekwueme, C.I. Abanobi, R.C. Eluagu, I.J.I.J.o.O. Chemazu, Gas and C. Engineering, Evaluation of the Economic Potentials of a Mini Gas-to-Liquids (GTL) Plant in Nigeria. 9 (2021) 98. [Crossref], [Google scholar], [Publisher]
10. Molnar G. Economics of gas transportation by pipeline and LNG. InThe Palgrave Handbook of International Energy Economics 2022 May 28 (pp. 23-57). Cham: Springer International

Publishing. [Crossref], [Google scholar], [Publisher]
11. Chen C, Li C, Reniers G, Yang F. Safety and security of oil and gas pipeline transportation: A systematic analysis of research trends and future needs using WoS, *Journal of Cleaner Production*; 2021 Jan 10; 279:123583. [Crossref], [Google scholar], [Publisher]
12. Javanmardi J, Nasrifar K, Najibi SH, Moshfeghian M. Economic evaluation of natural gas hydrate as an alternative for natural gas transportation, *Applied Thermal Engineering*; 2005 Aug 1; 25(11-12):1708-23. [Crossref], [Google scholar], [Publisher]
13. Hao W, Wang J, Fan S, Hao W. Evaluation and analysis method for natural gas hydrate storage and transportation processes, *Energy conversion and management*; 2008 Oct 1; 49(10):2546-53. [Crossref], [Google scholar], [Publisher]
14. Mimachi H, Takeya S, Yoneyama A, Hyodo K, Takeda T, Gotoh Y, Murayama T. Natural gas storage and transportation within gas hydrate of smaller particle: Size dependence of self-preservation phenomenon of natural gas hydrate, *Chemical Engineering Science*; 2014 Oct 18; 118:208-13. [Crossref], [Google scholar], [Publisher]
15. Xia Z, Zhao Q, Chen Z, Li X, Zhang Y, Xu C, Yan K. Review of methods and applications for promoting gas hydrate formation process, *Journal of Natural Gas Science and Engineering*; 2022 May 1; 101:104528. [Crossref], [Google scholar], [Publisher]
16. Koh CA, Sloan ED, Sum AK, Wu DT. Fundamentals and applications of gas hydrates, *Annual review of chemical and biomolecular engineering*; 2011 Jul 15; 2:237-57. [Crossref], [Google scholar], [Publisher]
17. Makogon YF. Natural gas hydrates–A promising source of energy, *Journal of natural gas science and engineering*; 2010 Mar 1; 2(1):49-59. [Crossref], [Google scholar], [Publisher]
18. A. Mohammadi, The Adverse Effect of SDS on the Growth Rate of Double Tetra n-butylammonium Chloride + Methane Semiclathrate Hydrate. *Progress in Chemical and Biochemical Research*, (2023) [Crossref], [Google scholar], [Publisher]
19. He Y, Sun MT, Chen C, Zhang GD, Chao K, Lin Y, Wang F. Surfactant-based promotion to gas hydrate formation for energy storage, *Journal of Materials Chemistry A*; 2019; 7(38):21634-61. [Crossref], [Google scholar], [Publisher]
20. Both AK, Gao Y, Zeng XC, Cheung CL. Gas hydrates in confined space of nanoporous materials: new frontier in gas storage technology, *Nanoscale*; 2021; 13(16):7447-70. [Crossref], [Google scholar], [Publisher]
21. Pahlavanzadeh H, Javidani AM, Ganji H, Mohammadi A. Investigation of the Effect of NaCl on the Kinetics of R410a Hydrate Formation in the Presence and Absence of Cyclopentane with Potential Application in Hydrate-based Desalination, *Industrial & Engineering Chemistry Research*; 2020 Jul 14; 59(31):14115-25. [Crossref], [Google scholar], [Publisher]
22. Khan MN, Peters CJ, Koh CA. Desalination using gas hydrates: The role of crystal nucleation, growth and separation, *Desalination*; 2019 Oct 15; 468:114049. [Crossref], [Google scholar], [Publisher]
23. Zhang Q, Zheng J, Zhang B, Linga P. Coal mine gas separation of methane via clathrate hydrate process aided by tetrahydrofuran and amino acids, *Applied Energy*; 2021 Apr 1; 287:116576. [Crossref], [Google scholar], [Publisher]
24. Gambelli AM, Castellani B, Nicolini A, Rossi F. Gas hydrate formation as a strategy for CH4/CO2 separation: Experimental study on gaseous mixtures produced via Sabatier reaction, *Journal of Natural Gas Science and Engineering*; 2019 Nov 1; 71:102985. [Crossref], [Google scholar], [Publisher]
25. Mohammadi A. The roles TBAF and SDS on the kinetics of methane hydrate formation as a cold

storage material, *Journal of Molecular Liquids*; 2020 Jul 1; 309:113175. [Crossref], [Google scholar], [Publisher]

26. Mohammadi A, Jodat A. Investigation of the kinetics of TBAB+ carbon dioxide semiclathrate hydrate in presence of tween 80 as a cold storage material, *Journal of Molecular Liquids*; 2019 Nov 1; 293:111433. [Crossref], [Google scholar], [Publisher]
27. Srivastava S, Hitzmann B, Zettel V. A future road map for carbon dioxide (CO2) gas hydrate as an emerging technology in food research, *Food and Bioprocess Technology*; 2021 Sep; 14(9):1758-62. [Crossref], [Google scholar], [Publisher]
28. Safari S, Varaminian F. Study the kinetics and thermodynamics conditions for CO2 hydrate formation in orange juice concentration, *Innovative Food Science & Emerging Technologies*; 2019 Oct 1; 57:102155. [Crossref], [Google scholar], [Publisher]
29. Javidani AM, Abedi-Farizhendi S, Mohammadi A, Mohammadi AH, Hassan H, Pahlavanzadeh H. Experimental study and kinetic modeling of R410a hydrate formation in presence of SDS, tween 20, and graphene oxide nanosheets with application in cold storage, *Journal of Molecular Liquids*; 2020 Apr 15; 304:112665. [Crossref], [Google scholar], [Publisher]
30. Mohammadi A, Babakhanpour N, Javidani AM, Ahmadi G. Corn's dextrin, a novel environmentally friendly promoter of methane hydrate formation, *Journal of Molecular Liquids*; 2021 Aug 15; 336:116855. [Crossref], [Google scholar], [Publisher]
31. Mohammadi A. The roles TBAF and SDS on the kinetics of methane hydrate formation as a cold storage material, *Journal of Molecular Liquids*; 2020 Jul 1; 309:113175. [Crossref], [Google scholar], [Publisher]
32. Sadeh E, Farhadian A, Mohammadi A, Maddah M, Pourfath M, Yang M. Energy-efficient storage of methane and carbon dioxide capture in the form of clathrate hydrates using a novel non-foaming surfactant: An experimental and computational investigation, *Energy Conversion and Management*; 2023 Oct 1; 293:117475. [Crossref], [Google scholar], [Publisher]
33. Khan MS, Partoon B, Bavoh CB, Lal B, Mellon NB. Influence of tetramethylammonium hydroxide on methane and carbon dioxide gas hydrate phase equilibrium conditions, *Fluid Phase Equilibria*; 2017 May 25; 440:1-8. [Crossref], [Google scholar], [Publisher]
34. Zhong DL, Li Z, Lu YY, Sun DJ. Phase equilibrium data of gas hydrates formed from a CO2+ CH4 gas mixture in the presence of tetrahydrofuran, *Journal of Chemical & Engineering Data*; 2014 Dec 11; 59(12):4110-7. [Crossref], [Google scholar], [Publisher]
35. Bozorgian A, Arab Aboosadi Z, Mohammadi A, Honarvar B, Azimi AR. Statistical Analysis of the Effects of Aluminum Oxide (Al2O3) Nanoparticle, TBAC, and APG on Storage Capacity of CO2 Hydrate Formation, *Iranian Journal of Chemistry and Chemical Engineering*; 2022 Jan 1; 41(1):220-31. [Crossref], [Google scholar], [Publisher]
36. Bozorgian A, Aboosadi ZA, Mohammadi A, Honarvar B, Azimi A. Determination of CO2 gas hydrates surface tension in the presence of nonionic surfactants and TBAC, *Revue Roumaine de Chimie*; 2020 Dec 1; 65:1061-5. [Crossref], [Google scholar], [Publisher]
37. Bozorgian A, Arab Aboosadi Z, Mohammadi A, Honarvar B, Azimi A. Evaluation of the effect of nonionic surfactants and TBAC on surface tension of CO2 gas hydrate, *Journal of Chemical and Petroleum Engineering*; 2020 Jun 1; 54(1):73-81. [Crossref], [Google scholar], [Publisher]
38. Zhang JS, Lee S, Lee JW. Kinetics of methane hydrate formation from SDS solution, *Industrial & Engineering Chemistry Research*; 2007 Sep 12; 46(19):6353-9. [Crossref], [Google scholar], [Publisher]
39. Liu X, Ren J, Chen D, Yin Z. Comparison of SDS and L-Methionine in promoting CO2 hydrate

kinetics: Implication for hydrate-based CO_2 storage, *Chemical Engineering Journal*; 2022 Jun 15; 438:135504. [Crossref], [Google scholar], [Publisher]

40. Sun Z, Wang R, Ma R, Guo K, Fan S. Effect of surfactants and liquid hydrocarbons on gas hydrate formation rate and storage capacity, *International journal of energy research*; 2003 Jun 25; 27(8):747-56. [Crossref], [Google scholar], [Publisher]
41. Karaaslan U, Parlaktuna M. Surfactants as hydrate promoters?, *Energy & Fuels*; 2000 Sep 18; 14(5):1103-7. [Crossref], [Google scholar], [Publisher]
42. Abedi-Farizhendi S, Iranshahi M, Mohammadi A, Manteghian M, Mohammadi AH. Kinetic study of methane hydrate formation in the presence of carbon nanostructures, *Petroleum Science*; 2019 Jun; 16:657-68. [Crossref], [Google scholar], [Publisher]
43. Mohammadi A, Manteghian M, Mohammadi AH, Jahangiri A. Induction time, storage capacity, and rate of methane hydrate formation in the presence of SDS and silver nanoparticles, *Chemical engineering communications*; 2017 Dec 2; 204(12):1420-7. [Crossref], [Google scholar], [Publisher]
44. Arjang S, Manteghian M, Mohammadi A. Effect of synthesized silver nanoparticles in promoting methane hydrate formation at 4.7 MPa and 5.7 MPa, *Chemical Engineering Research and Design*; 2013 Jun 1; 91(6):1050-4. [Crossref], [Google scholar], [Publisher]
45. Hassan H, Javidani AM, Mohammadi A, Pahlavanzadeh H, Abedi-Farizhendi S, Mohammadi AH. Effects of Graphene Oxide Nanosheets and Al_2O_3 Nanoparticles on CO_2 Uptake in Semi-clathrate Hydrates, *Chemical Engineering & Technology*; 2021 Jan; 44(1):48-57. [Crossref], [Google scholar], [Publisher]
46. Javidani AM, Abedi-Farizhendi S, Mohammadi A, Hassan H, Mohammadi AH, Manteghian M. The effects of graphene oxide nanosheets and Al2O3 nanoparticles on the kinetics of methane+ THF hydrate formation at moderate conditions, *Journal of Molecular Liquids*; 2020 Oct 10; 316:113872. [Crossref], [Google scholar], [Publisher]
47. Peng DY, Robinson DB. A new two-constant equation of state, *Industrial & Engineering Chemistry Fundamentals*; 1976 Feb; 15(1):59-64. [Crossref], [Google scholar], [Publisher]
48. Mohammadi A, Manteghian M, Haghtalab A, Mohammadi AH, Rahmati-Abkenar M. Kinetic study of carbon dioxide hydrate formation in presence of silver nanoparticles and SDS, *Chemical engineering journal*; 2014 Feb 1; 237:387-95. [Crossref], [Google scholar], [Publisher]
49. Lv X, Lu D, Liu Y, Zhou S, Zuo J, Jin H, Shi B, Li E. Study on methane hydrate formation in gas–water systems with a new compound promoter, *RSC advances*; 2019; 9(57):33506-18. [Crossref], [Google scholar], [Publisher]
50. Lee S, Zhang J, Mehta R, Woo TK, Lee JW. Methane hydrate equilibrium and formation kinetics in the presence of an anionic surfactant, *The Journal of Physical Chemistry C*; 2007 Mar 29; 111(12):4734-9. [Crossref], [Google scholar], [Publisher]
51. Molokitina NS, Nesterov AN, Podenko LS, Reshetnikov AM. Carbon dioxide hydrate formation with SDS: Further insights into mechanism of gas hydrate growth in the presence of surfactant, *Fuel*; 2019 Jan 1; 235:1400-11. [Crossref], [Google scholar], [Publisher]